2009

Characterizing forest succession with lidar data: An evaluation for the Inland Northwest, USA

Michael J. Falkowski
Michigan Technological University, mjfalkow@mtu.edu

Jeffrey S. Evans
The Nature Conservancy, jeffrey_evans@tnc.org

Sebastián Martinuzzi
University of Idaho, smartinuzzi@vandals.uidaho.edu

Paul E. Gessler
University of Idaho, paulg@uidaho.edu

Andrew T. Hudak
Rocky Mountain Research Station, ahudak@fs.fed.us

Remote Sensing of Environment 113 (2009) 946–956

Contents lists available at ScienceDirect

Remote Sensing of Environment

journal homepage: www.elsevier.com/locate/rse

Characterizing forest succession with lidar data: An evaluation for the Inland Northwest, USA

Michael J. Falkowski [a,c,*], Jeffrey S. Evans [b], Sebastian Martinuzzi [c], Paul E. Gessler [c], Andrew T. Hudak [d]

[a] Pacific Forestry Centre, Canadian Forest Service, Natural Resources Canada, 506 West Burnside Road, Victoria, Canada BC V8Z 1M5
[b] The Nature Conservancy, Rocky Mountain Conservation Region, 117 East Mountain Avenue, Suite 201 Fort Collins, CO 80534, USA
[c] Geospatial Laboratory for Environmental Dynamics, Department of Forest Resources, University of Idaho, Moscow, ID 83843, USA
[d] USDA Forest Service, Rocky Mountain Research Station, 1221 S. Main St. Moscow, ID 83843, USA

ARTICLE INFO

Article history:
Received 28 March 2008
Received in revised form 6 January 2009
Accepted 16 January 2009

Keywords:
Lidar
Forest succession
Forest structure
Random forests
Wildlife

ABSTRACT

Quantifying forest structure is important for sustainable forest management, as it relates to a wide variety of ecosystem processes and services. Lidar data have proven particularly useful for measuring or estimating a suite of forest structural attributes such as canopy height, basal area, and LAI. However, the potential of this technology to characterize forest succession remains largely untested. The objective of this study was to evaluate the use of lidar data for characterizing forest successional stages across a structurally diverse, mixed-species forest in Northern Idaho. We used a variety of lidar-derived metrics in conjunction with an algorithmic modeling procedure (Random Forests) to classify six stages of three-dimensional forest development and achieved an overall accuracy>95%. The algorithmic model presented herein developed ecologically meaningful classifications based upon lidar metrics quantifying mean vegetation height and canopy cover, among others. This study highlights the utility of lidar data for accurately classifying forest succession in complex, mixed coniferous forests; but further research should be conducted to classify forest successional stages across different forests types. The techniques presented herein can be easily applied to other areas. Furthermore, the final classification map represents a significant advancement for forest succession modeling and wildlife habitat assessment.

1. Introduction

Quantification of forest structure is critical for sustainable forest management (O'Hara et al., 1996) as it relates to a wide variety of ecosystem processes and services, including gas exchange, productivity, biodiversity, and water interception (Deguchi et al., 2006; Fuller et al., 2007; Law et al., 2001; Roland & Taylor, 1997). Forest structure can be quantified in myriad ways including the prediction of individual components of structure (*e.g.* leaf area index, aboveground biomass, basal area; Clark et al., 2008; Coops et al., 2007; Saatchi et al., 2007), or through measuring three-dimensional attributes related to forest succession (Bergen & Dronova, 2007; Hao et al., 2007). Light detection and ranging (lidar) data have proven particularly useful for estimating a suite of forest structural attributes such as canopy height, biomass, basal area, and LAI (Coops et al., 2007; Dubayah & Drake, 2000; Lefsky et al., 1999; Nelson et al., 1988; Roberts et al., 2005; White et al., 2000).

In terms of forest management, selecting which approach to use is dependent upon specific management objectives as well as the time scale of interest. For example, at short time scales (monthly to inter-annual) measuring or predicting specific forest structural characteristics (*e.g.*, leaf area index) may be sufficient for gaining an understanding of forest processes such as diurnal or annual carbon flux. However, at longer temporal scales (decade- to century-scales) successional dynamics become the primary drivers of many forest processes, hence measuring three-dimensional structural attributes related to forest succession and stand development is important for predicting processes such as long-term carbon sequestration (Shugart, 2000). Furthermore, accurate classifications of forest succession that cover large spatial extents are critical to achieving many goals of sustainable forest management. For example, classifications of forest succession can be used to characterize wildlife habitat (Cody, 1985; Helle, 1985; Helle & Monkkonen, 1990) and future forest conditions via forest succession models (Busing et al., 2007; Shugart, 2000; Vargas et al., 2008).

Forest successional stage can be directly assessed in the field via traditional forest inventory techniques. Although accurate, field-based classifications of forest succession are often limited to small spatial extents (Bergen & Dronova, 2007). In order to be useful for sustainable forest management, classifications of forest succession must cover large areas. The synoptic data provided by remote sensing instruments have provided a means to characterize forest successional stage across large spatial extents (Song et al., 2007). Indeed, data collected by optical

* Corresponding author. Tel.: +1 250 363 0780.
E-mail address: mjfalkowski@vandals.uidaho.edu (M.J. Falkowski).

0034-4257/$ – see front matter © 2009 Elsevier Inc. All rights reserved.
doi:10.1016/j.rse.2009.01.003

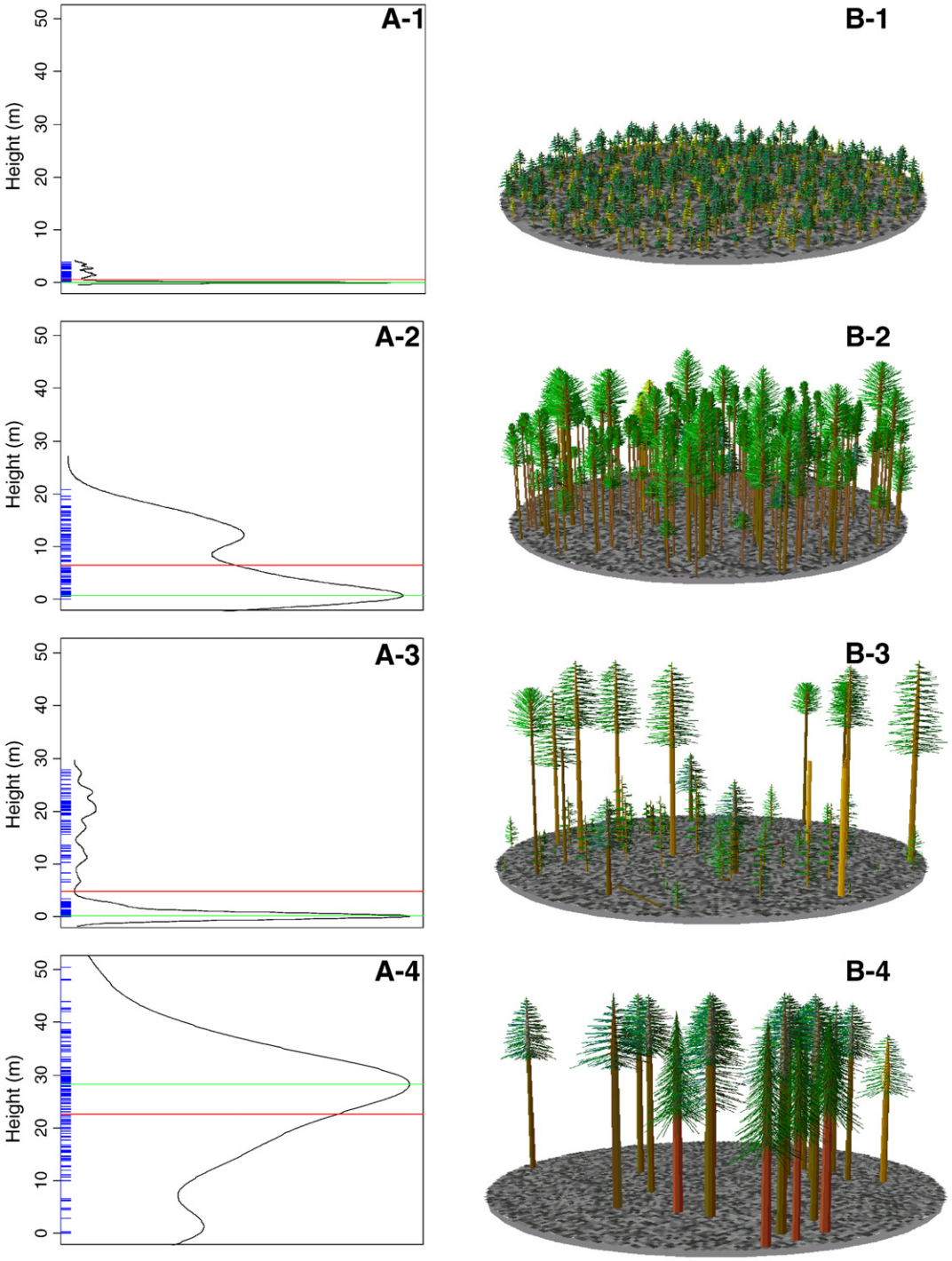

Fig. 1. Hypothetical discrete return lidar pulse height distributions (A-1:A-4) and corresponding forest successional stages (B-1:B-4). (A-1:A-4) Lidar pulse height distributions within a forest inventory plot. The black line is the probability density function. The red and green lines represent the mean and modal lidar height, respectively. The blue tic marks on the *y*-axis correspond to the height in meters of individual lidar returns. (B-1:B-4) Graphical depictions of four different forest successional stages: stand initiation (B-1), young multistory (B-2), understory reinitiation (B-3), and old multistory (B-4). (For interpretation of the references to color in this figure legend, the reader is referred to the web version of this article.)

sensors have been used to classify forest succession or predict stand age with varying degrees of accuracy (Bergen & Dronova, 2007; Cohen et al., 1995; Falkowski et al., 2005; Miller et al., 2003; Song & Woodcock, 2002). However, forest succession is a three-dimensional process, and passive optical sensors are much less sensitive to three-dimensional canopy structure than lidar instruments.

Since lidar actively measures the three-dimensional arrangement of forest canopies, providing accurate and precise estimates of forest structural attributes, it has the potential to classify forest succession across large spatial extents. Lidar metrics characterizing the distribution and density of vegetation within forest inventory plots differ depending upon the corresponding successional stage, making it possible to classify forest successional stages via lidar data. For example, in a forest undergoing stand initiation, the majority of lidar pulse returns (Fig. 1A-1 and B-1) are reflected off of or near the ground surface, with few reflecting off of seedlings and saplings (height < 3 m). In a young multistory forest (Fig. 1A-2 and B-2) lidar pulse returns exhibit a multi-modal distribution, with one mode occurring at the

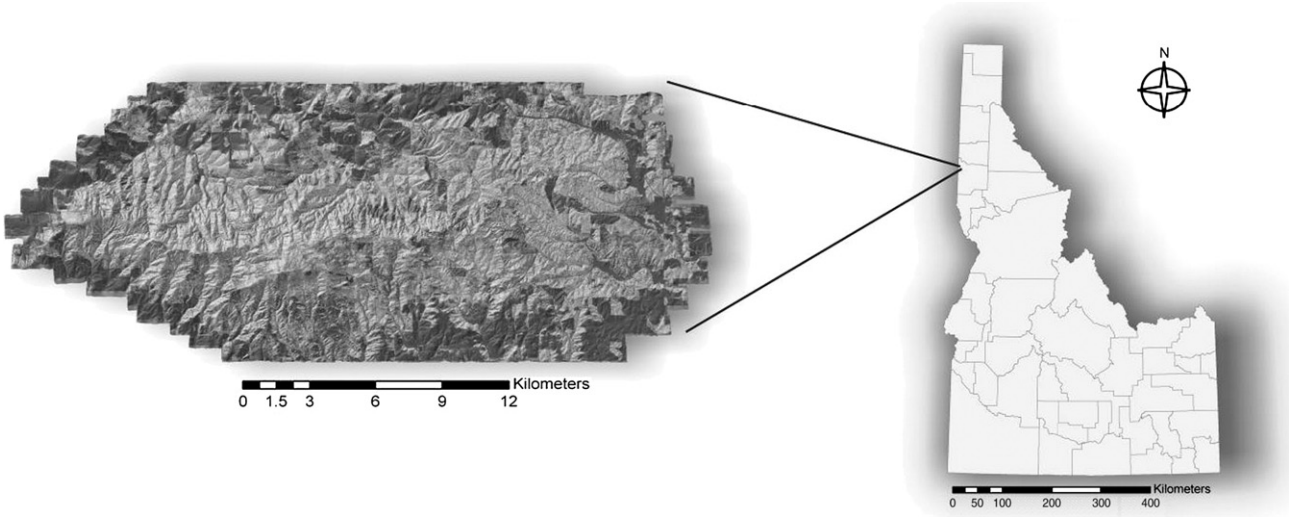

Fig. 2. The Palouse Range study area (46° 48′ N; 116° 52′ W). A lidar derived canopy height layer overlaid with a hillshade layer derived from the lidar digital elevation model.

ground surface and others in the forest canopy (height ~10–20 m). As the forest transitions into more advanced stages of succession, the distribution of lidar pulse returns within an inventory plot change dramatically. Thus, lidar height metrics characterizing the distribution and density of forest vegetation should prove particularly useful in the classification of forest successional stage.

The few studies that have used lidar data to classify forest successional stage have been limited to differentiating between two successional classes, a single story class and a multi-story class (Zimble et al., 2003), or have used an integration of hyperspectral imagery and lidar data to classify structure-based cover type classes (Hill & Thomson, 2005). To be useful for quantifying ecological processes and wildlife habitat relationships, and to benefit sustainable forest management, classifications of forest succession must be grounded in the dynamics of stand development and reflect all potential stages of forest development (O'Hara et al., 1996).

The objective of this study is to use discrete return lidar to classify forest successional stage across a structurally diverse, mixed-species forest in Northern Idaho, USA. Specifically, we focus upon using various lidar height metrics to classify forest successional stage according to a classification scheme specifically developed for forests of the Inland Northwest, USA (O'Hara et al., 1996). In addition to classifying forest successional stage, we use an algorithmic modeling procedure to (i) determine the most important lidar metrics for classifying forest successional stage and (ii) select the most parsimonious classification model while retaining the highest degree of classification accuracy as possible. Classification performance is evaluated via traditional accuracy assessment statistics, and by determining if the algorithmic model produced logical, ecologically meaningful classifications. Furthermore, a spatial assessment of classification uncertainty is conducted to explore potential limitations of using lidar data to classify forest successional stage across structurally diverse forested regions.

2. Methods

2.1. Study area and data collection

The focal area of our study is the Palouse Range (~30,000 ha; Latitude 46° 48′ N, Longitude 116° 52′ W), which lies at the extreme western extent of the Clearwater Mountains in Northern Idaho, USA (Fig. 2). The Palouse Range is topographically complex and primarily comprised of temperate mixed-conifer forest. Dominant tree species across this study area include: *Pinus ponderosa* C. Lawson var. *scopulorum* Engelm., *Pseudotsuga menziesii* (Mirb.) Franco var. *glauca* (Beissn.) Franco, *Abies grandis* (Douglas ex D. Don) Lindl., *Thuja plicata* Donn ex D. Don, and *Larix occidentalis* Nutt. Timber companies own a majority of the land, but there also are many private and public land holdings. This includes a large tract of experimental forestland, owned by the University of Idaho, and a small parcel formerly owned by The Nature Conservancy, which is protected for biodiversity conservation. The unique management goals and strategies of each of these landowners, coupled with the regions topographic complexity, have created a forest that is diverse in species composition, forest age, and structure, making it an ideal location to test the utility of lidar data for the classification of forest successional stage.

Eighty-one forest inventory plots were located across the study area using a stratified systematic sampling protocol. The study area was stratified into nine unique combinations of elevation and solar insolation. Inventory plots were then systematically selected within each stratum based upon a Landsat-derived leaf area index layer (Pocewicz et al., 2004). Since elevation and solar insolation influence forest productivity and species composition, and LAI describes current forest canopy conditions, employing theses strata ensured that the eighty-one forest inventory plots covered the full range of forest species composition and canopy structure conditions across the study area.

During the summer of 2003, a 404.69 m^2 fixed-radius (11.35 m radius) forest inventory plot was installed at each sample location. The diameter at breast height (DBH), species, height, as well as distance and bearing from plot center, was measured and recorded for each tree (DBH>2.7 cm) falling within the fixed radius plot. Seedlings and saplings were also measured and tallied across the entire inventory plot. Falkowski et al. (2005) provide additional details regarding the sampling design and data collection protocols.

2.2. Forest successional stage classification scheme

Using a rule-based classification procedure presented by O'Hara et al. (1996), each of the eighty-one forest inventory plots was categorized into the appropriate forest successional stage based upon the forest inventory field data. The classification scheme was specifically developed for forests of the Inland Northwest, USA, and recognizes seven different structural stages of forest succession; stand initiation, open stem exclusion, closed stem exclusion, understory reinitiation, young multi-strata, old forest multi-strata, and old forest single-stratum. O'Hara et al. (1996) present detailed

Table 1
Forest successional stage class descriptions adapted from O'Hara et al. (1996).

Class	Description	Number of plots in class
Open	Treeless or one broken stratum of trees or shrubs present. Limited establishment of new individuals.	9
Stand Initiation (SI)	Growing space reoccupied by seedlings, saplings, or shrubs following stand replacing disturbance.	7
Understory Reinitiation (UR)	Older cohort of trees being replaced by new individuals. Broken overstory with an understory stratum present.	7
Young Multistory (YMS)	Two or more cohorts of trees from a variety of age-classes. No large or medium trees present	30
Mature Multistory (MMS)	Two or more cohorts of trees from a variety of age-classes. Medium trees present. Large trees absent	11
Closed Stem Exclusion (CSE)	One closed canopy stratum present. Limited establishment of new individuals due to low light availability in the understory.	11
Old Multistory (OMS)	Two or more cohorts of trees from a variety of age-classes. Dominated by large trees.	6

sional stage classes. For the purpose of this study, the aforementioned categories were slightly modified to reflect the successional stages present across the Palouse Range study area (Table 1). Specifically, an 'Open' class was added to account for areas within the Palouse Range study area that do not support tree growth (*e.g.*, agricultural lands near the forest boundary and wet meadows within the forested area). Furthermore, the Old Forest Single-Stratum class presented by O'Hara et al. (1996) was eliminated because the structural stage is not present across the Palouse Range study area. Table 1 presents verbal descriptions of the forest successional stages found across the Palouse Range.

2.3. Lidar acquisition and processing

Discrete return lidar data (~1.95 m nominal post spacing; ~0.26 lidar pulses per m^2) were acquired in summer 2003 across the entire study area with an Optech ALTM30 system owned and operated by Horizons, Incorporated (http://www.horizonsinc.com/). The system operated at a wavelength of 1064 nm and was flown at approximately 2500 m above terrain elevation. Once acquired, the lidar data were separated into ground and non-ground returns using the Multi-scale Curvature Classification algorithm (Evans & Hudak, 2007). Following classification, a high resolution (1 m) digital elevation model (DEM) was created from the ground returns using an iterative finite difference (IFD) interpolation algorithm employed by the ArcInfo TOPOGRID module. The interpolated DEM had root mean square error (RMSE) of 0.306 m and 0.166 m in high canopy cover and low canopy cover forests, respectively (Evans & Hudak, 2007).

The height above ground surface was then calculated for all non-ground returns through DEM subtraction. For the purpose of this study, the lidar data were aggregated into 20 m bins (*i.e.*, grid cells) approximately the same size as the forest inventory plots. A variety of candidate classification variables were calculated from all non-ground lidar returns (height>0) within every 20 m bin. These variables included the percentage of lidar returns within seven defined canopy height strata, and twenty-one statistics characterizing the statistical distribution of lidar heights within each 20 m bin. Canopy cover was also included, and calculated as the percentage of total returns that were above 1 m in height. Other lidar height metrics included a texture variable and the percentage of 1st, 2nd, 3rd, and non-ground lidar returns within each 20 m bin. In total, thirty-four candidate predictor variables, which have proved useful for characterizing forest structure (Hudak et al., 2006, 2008), were generated (Table 2).

2.4. Data analysis

2.4.1. The Random Forest classification algorithm

For the purpose of this study, we used the Random Forest (RF) algorithm (Breiman, 2001) to classify forest successional stage based upon the thirty-four candidate Lidar height metrics (Table 2). The RF algorithm is a classification tree technique that has achieved excellent results in classifying remotely sensed data (Hudak et al., 2008; Lawrence et al., 2006). Classification tree algorithms are commonly used to classify remotely sensed data (*e.g.,* Coops et al., 2006; Falkowski et al., 2005; Lawrence & Wright, 2001) because they are easily interpretable, can produce accurate results, and can handle categorical and continuous data simultaneously (Breiman et al., 1984; Cutler et al., 2007). The major advantages of the RF classification tree algorithm over traditional classification tree techniques are: (1) through a bootstrap approach it can achieve substantially higher accuracies than single classification tree methods, while simultaneously addressing over-fitting problems associated with traditional classification tree models, (2) it develops robust (accurate and unbiased) predictions based on votes across bootstrap replicates, (3) it is nonparametric and thus unaffected by distributional assumptions, (4) the GENI statistic used for node splitting can integrate non-linear variable interactions, and (5) it provides a reliable, internal estimate of classification accuracy (Breiman, 2001; Cutler et al., 2007; Lawrence et al., 2006; Prasad et al., 2006). The RF algorithm develops classifications by growing numerous (100 s to >1000 s) classification trees from a random subset of training data (approximately 63% random subset), while randomly permuting predictor variables at each node (*e.g.*, Table 2). The correct classifications, or predictions, are then determined by selecting the most common classification result at

Table 2
Lidar metrics used in the classification.

Metric name	Metric description
HMIN	Minimum Height
HMAX[a]	Maximum Height
HRANGE	Range of Heights
HMEAN[a,b]	Mean Height
HMEDIAN[a,b]	Median Height
HMODE[b]	Modal Height
NMODES	Number of Modes
HAAD	Average Absolute Deviation of Heights
HMAD	Median Absolute Deviation of Heights
HSTD	Standard Deviation of Heights
HVAR	Variance of Heights
HSKEW	Skewness of Heights
HKURT	Kurtosis of Heights
HCV	Coefficient of Variation of Heights
H05PCT	Heights 5th Percentile
H10PCT	Heights 10th Percentile
H25PCT[b]	Heights 25th Percentile
H50PCT	Heights 50th Percentile (Median)
H75PCT[c]	Heights 75th Percentile
H90PCT	Heights 90th Percentile
H95PCT[c]	Heights 95th Percentile
CANOPY[a,b]	Canopy Cover (Vegetation Returns/Total Returns*100)
STRATUM0	Percentage of Ground Returns = 0 m
STRATUM1	Percentage of Non-Ground Returns>0 m and <=1 m
STRATUM2[b]	Percentage of Vegetation Returns>1 m and <=2.5 m
STRATUM3	Percentage of Vegetation Returns>2.5 m and <=10 m
STRATUM4[b]	Percentage of Vegetation Returns>10 m and <=20 m
STRATUM5[a,b]	Percentage of Vegetation Returns>20 m and <=30 m
STRATUM6	Percentage of Vegetation Returns>30 m
TEXTURE	Standard Deviation of Non-Ground Returns>0 m and <=1 m
PCT1	Percentage 1st Returns
PCT2	Percentage 2nd Returns
PCT3	Percentage 3rd Returns
NOTFIRST	Percentage 2nd or 3rd Returns

[a] Selected as an important variable in the 6 class model.
[b] Selected as an important variable in the 7 class model.
[c] Multi-collinear variable removed via QR decomposition.

each node within the group of multiple trees (Breiman, 2001; Lawrence et al., 2006; Prasad et al., 2006). Bootstrap error estimates and accuracies are calculated for each tree in the forest by classifying the portion of training data not selected for classification model development (approximately 37% of the training data). After all the trees in the forest are grown, overall error and accuracy is calculated by averaging error rates across all trees in the forest; this is analogous to cross-validated estimate of error and accuracy (Cutler et al., 2007). The algorithm also calculates the influence each predictor variable has upon model accuracy based upon the ratio of improvement in the mean squared error across bootstrap replicates, which can be used to determine the relative importance of each variable used in the classification. For this study, the RF algorithm was implemented as the RandomForest package (Liaw & Wiener, 2002) in the *R* statistical program (www.r-project.org; R Development Core Team, 2007).

2.4.2. Model selection and variable reduction

Although the RF algorithm is non-parametric, a model selection procedure (*i.e.*, variable reduction) was employed to select the optimal lidar variables to use in the classification of forest successional stage. The model selection procedure was formulated to develop the most parsimonious classification model, while retaining the highest possible classification accuracy. In order to reduce data redundancy and improve overall model interpretability, multi-collinear lidar classification variables were identified and removed via a multivariate variable screening process based upon Gram–Schmidt QR-Decomposition (Gentle et al., 2005; Golub & Van Loan, 1996). Classification variables were then automatically selected by iteratively running the RF algorithm and sub-setting classification variables based upon a mean square error ratio threshold. The final classification model is arrived at based on the criteria of smallest total and within class errors, and fewest numbers of classification variables. In order to stabilize individual class error, each RF model was run with 3000 bootstrap replicates (*i.e.*, individual classification trees).

2.4.3. Classification of forest successional stage

Two separate forest succession classifications were developed; a seven-class model containing all successional stage categories (Table 1), and a six-class model that aggregated the (MMS) and closed stem exclusion (CSE) classes. We chose to aggregate the MMS and CSE classes for two related reasons: (i) the only structural difference between the two classes is the presence (MMS) or absence (CSE) of seedlings and saplings in the forest understory, and (ii) that fact that the detection and identification of understory components in multi-story or closed canopy forests can be problematic with lidar data (Goodwin, 2006; Goodwin et al., 2007; Lee et al., 2004). Developing two separate classifications and comparing the results allowed us to explore this potential limitation.

2.4.4. Evaluation of classification accuracy and model performance

Classification accuracy was assessed based upon the bootstrap error estimates and error matrices calculated by the RF algorithm.

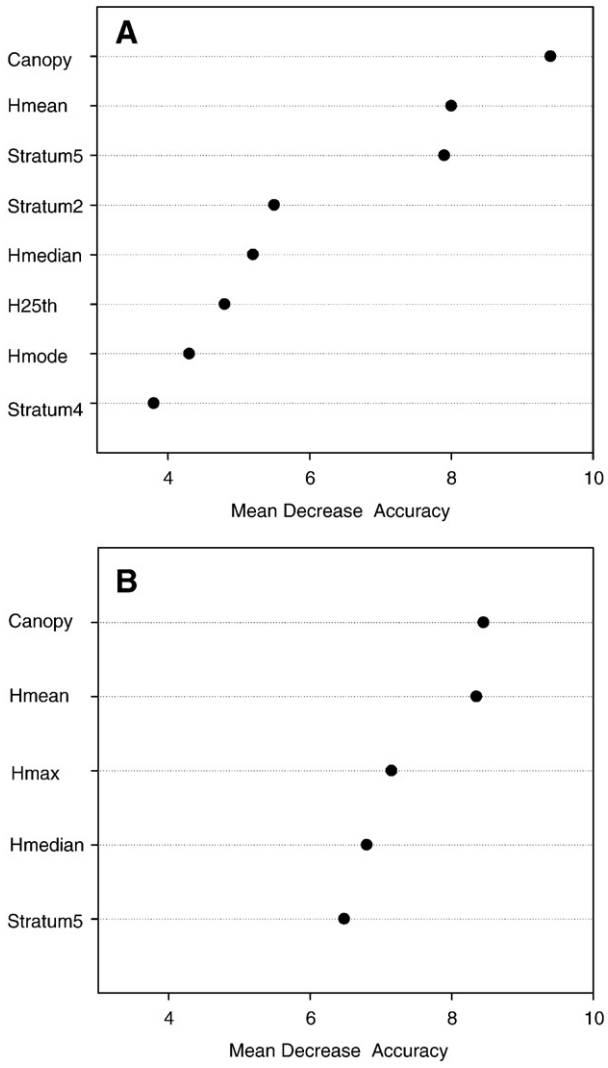

Fig. 3. Variable importance plots for the seven-class (A) and six-class (B) forest successional stage models. Units are the percent reduction in classification accuracy that would result from removing a given classification variable.

Overall accuracy, mean class accuracy, and errors of omission and commission were calculated and examined to assess the accuracy of each forest successional stage classification. In addition to the aforementioned error statistics, the uncertainty of successional stage classifications was evaluated by examining spatial predictions of maximum probability of occurrence for each class. To achieve this, a class probability was generated for each successional stage by treating the votes in the RF nodes matrix as a probability distribution. A separate map of class probability was then generated along with the individual class membership(s). Conditional density plots, which

Table 3
Classification accuracy statistics for the seven-class classification.

Class	Commission error	Omission error	Class accuracy
Open stem exclusion	0.00	11.11	88.89
Stand initiation	22.22	0.00	100.00
Understory initiation	0.00	14.29	85.71
Young multistory	0.00	3.33	96.67
Mature multistory	36.36	36.36	63.64
Closed stem exclusion	27.27	27.27	72.73
Old multistory	14.29	0.00	100.00
Overall accuracy	90.12		
Mean class accuracy	86.80		
K_{HAT}	84.51		

Table 4
Classification accuracy statistics for the six-class classification.

Class	Commission error	Omission error	Class accuracy
Open stem exclusion	0.00	0.00	100.00
Stand initiation	15.85	0.00	100.00
Understory initiation	0.00	14.29	85.71
Young multistory	0.00	3.33	96.67
Mature multistory	8.70	4.55	95.45
Old multistory	18.12	16.67	83.33
Overall accuracy	95.54		
Mean class accuracy	93.53		
K_{HAT}	93.48		

display the probability of each SS class occurring at a given level of each selected classification variable, were also examined to determine if the RF algorithm produced logical, ecologically meaningful classifications.

3. Results

3.1. Model selection

The QR decomposition procedure identified and removed two multi-collinear lidar metrics; the height of the 75th and 95th percentiles (Table 2). The model selection procedure (*i.e.,* variable reduction) identified eight lidar height variables to use for developing the seven-class forest successional stage classification model: mean height, median height, the modal height, 25th percentile height, canopy cover, and the density of the 2nd, 4th, and 5th strata (Table 2). For the six-class successional stage classification model, the model selection procedure (*i.e.,* variable selection) identified five lidar height variables to use for developing the classification: mean height, maximum height, median height, canopy cover, and the density of the 5th stratum (Table 2).

3.2. Classification accuracy and variable importance

The seven-class forest successional stage classification reported an overall accuracy of 90.12%, a mean class accuracy of 86.80%, and a K_{HAT} value of 84.5%. Individual class errors and omission and commission errors were low (Table 3). However, confusion did occur between the

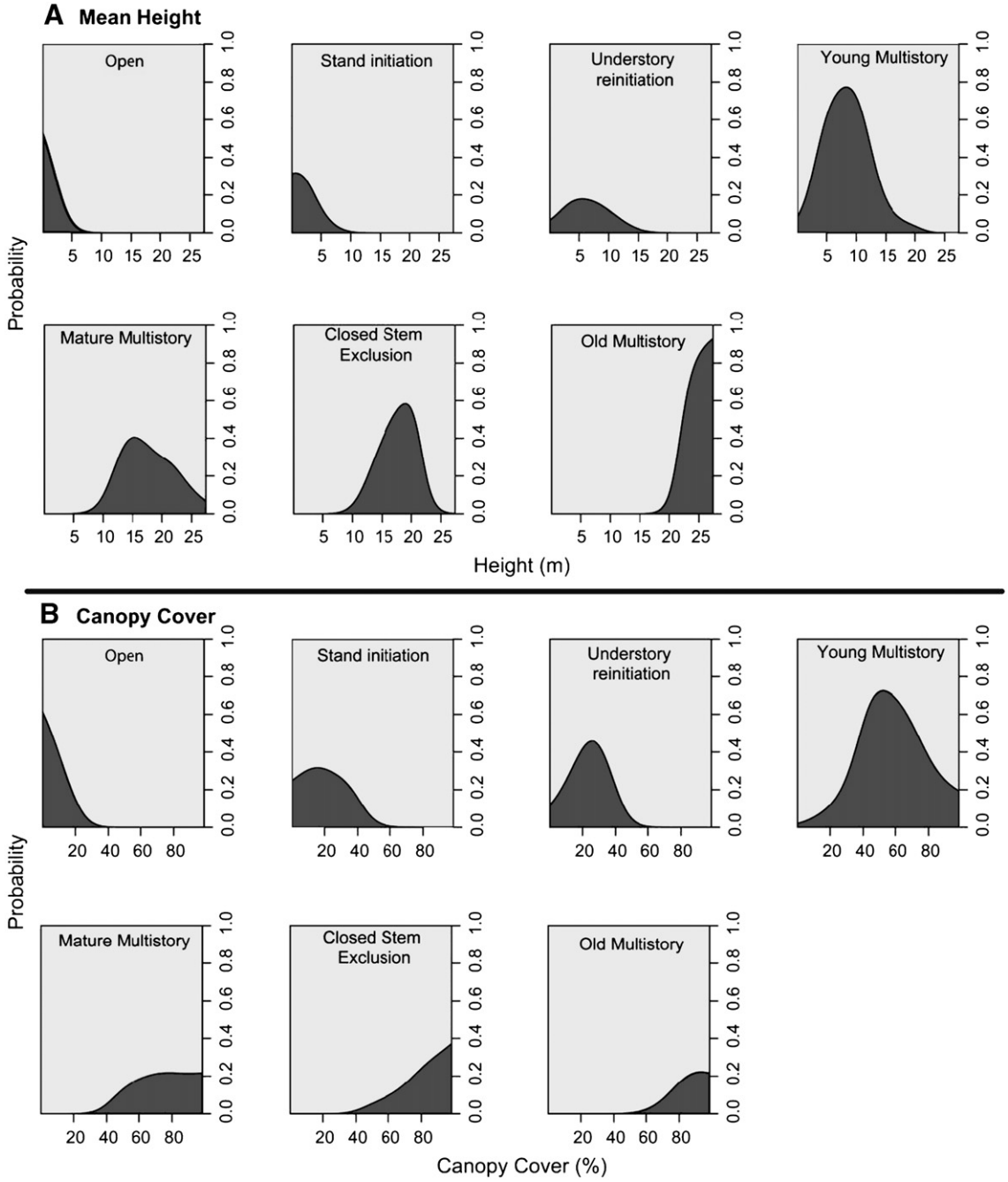

Fig. 4. Conditional density plots for the seven-class model. The gray region represents the presence of a particular class and the light grey background represents class absence. (A) The probability of the mean lidar height metric being in a particular class. The *x*-axis is height in meters and the *y*-axis is probability from 0–1. (B) The probability of the lidar derived canopy cover metric being in a particular class. The *x*-axis is in percent and the *y*-axis is probability from 0–1.

mature multistory (MMS) and closed stem exclusion (CSE) classes, which had individual class error rates of 27% and 36%, respectively. The model selection procedure (*i.e.*, variable selection) identified eight lidar metrics to use for developing the seven-class forest successional stage classification model (Table 2). In terms of variable importance, canopy cover, and mean height were the most important variables in the RF classification, followed by the density of the 2nd and 5th height strata, the median height, height of the 25th percentile, the modal height, and the density of the 4th stratum (Fig. 3).

Overall accuracy for six-class forest successional stage classification, which aggregated the MMS and CSE classes, was 95.54%, with mean class accuracy and K_{HAT} values of 93.53% and 93.48%, respectively (Table 4). Individual class errors, omission errors and commission errors were quite low (Table 4), and there was very little confusion between the individual classes. Again, the canopy cover and mean height lidar metrics were identified as the most important variables in the RF classification, followed by the maximum height, median height, and density of the 5th stratum (Fig. 3).

3.3. Model evaluation

Of the thirty-four candidate lidar metrics, only nine unique variables were selected as being important in both the seven- and six-class forest succession models (Table 2). Of these nine variables, canopy cover and mean lidar height were selected as the most important variables in both the seven- and six-class forest succession models (Fig. 3). Conditional density plots were examined to determine if the RF algorithm produced logical, ecologically meaningful

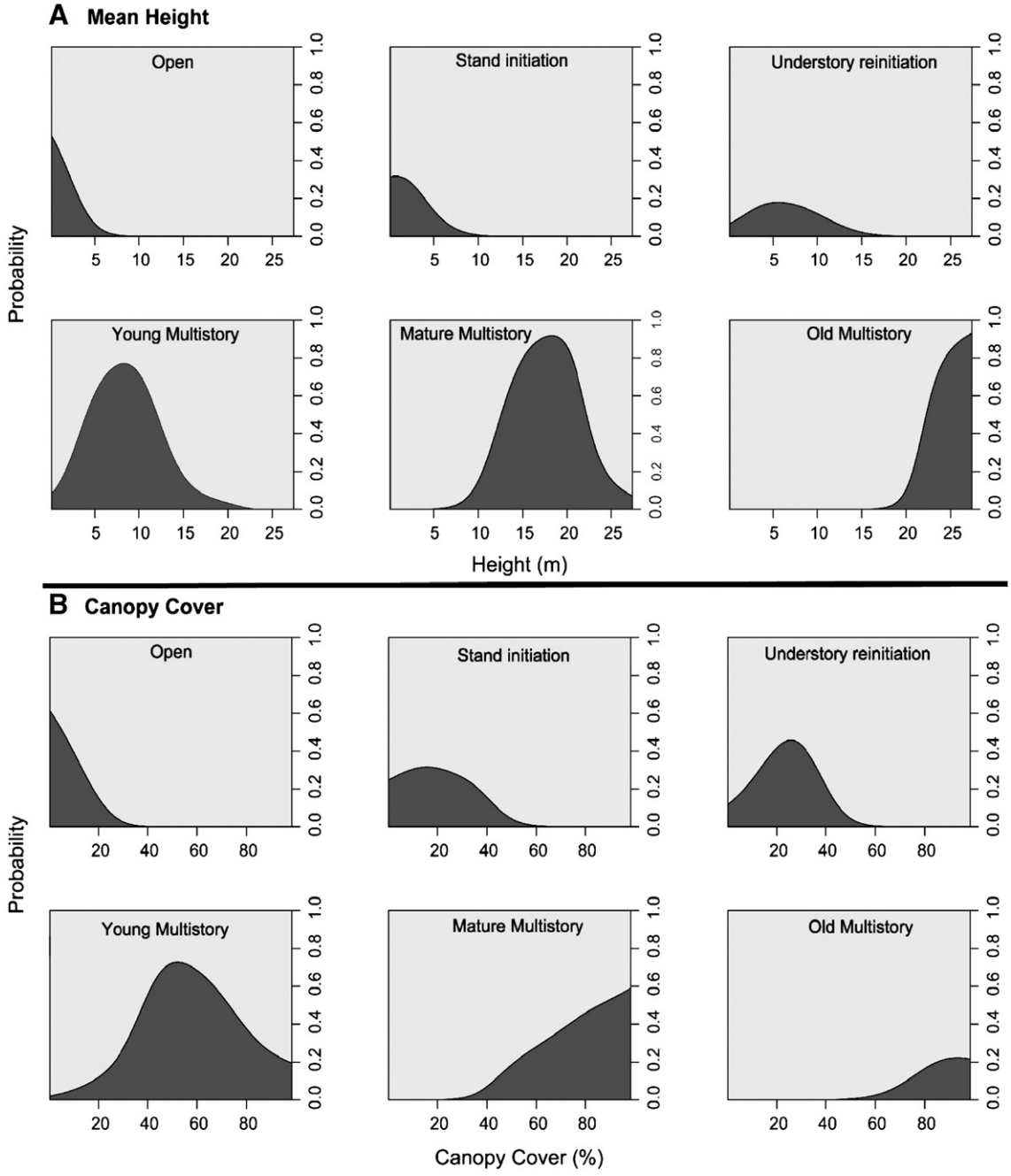

Fig. 5. Conditional density plots for the six-class model. The gray region represents the presence of a particular class and the light grey background represents class absence. (A) The probability of the mean lidar metric being in a particular class. The *x*-axis is height in meters and the *y*-axis is probability from 0–1. (B) The probability of the lidar derived canopy cover metric being in a particular class. The *x*-axis is in percent and the *y*-axis is probability from 0–1.

classifications. We only present the conditional density plots for the mean height and canopy cover lidar metrics (Figs. 4 and 5). For the seven- and six-class models, the peak of the conditional density plot of the mean lidar height metric increases as forests transition from early to advanced stages of succession. Canopy cover displays a similar trend; as succession advances canopy cover increases. However, when the forest is transitioning into the OMS class there is a slight reduction in canopy cover (Figs. 4 and 5).

The maximum probability of occurrence map (Fig. 6B), which was used to spatially assess successional stage prediction confidence

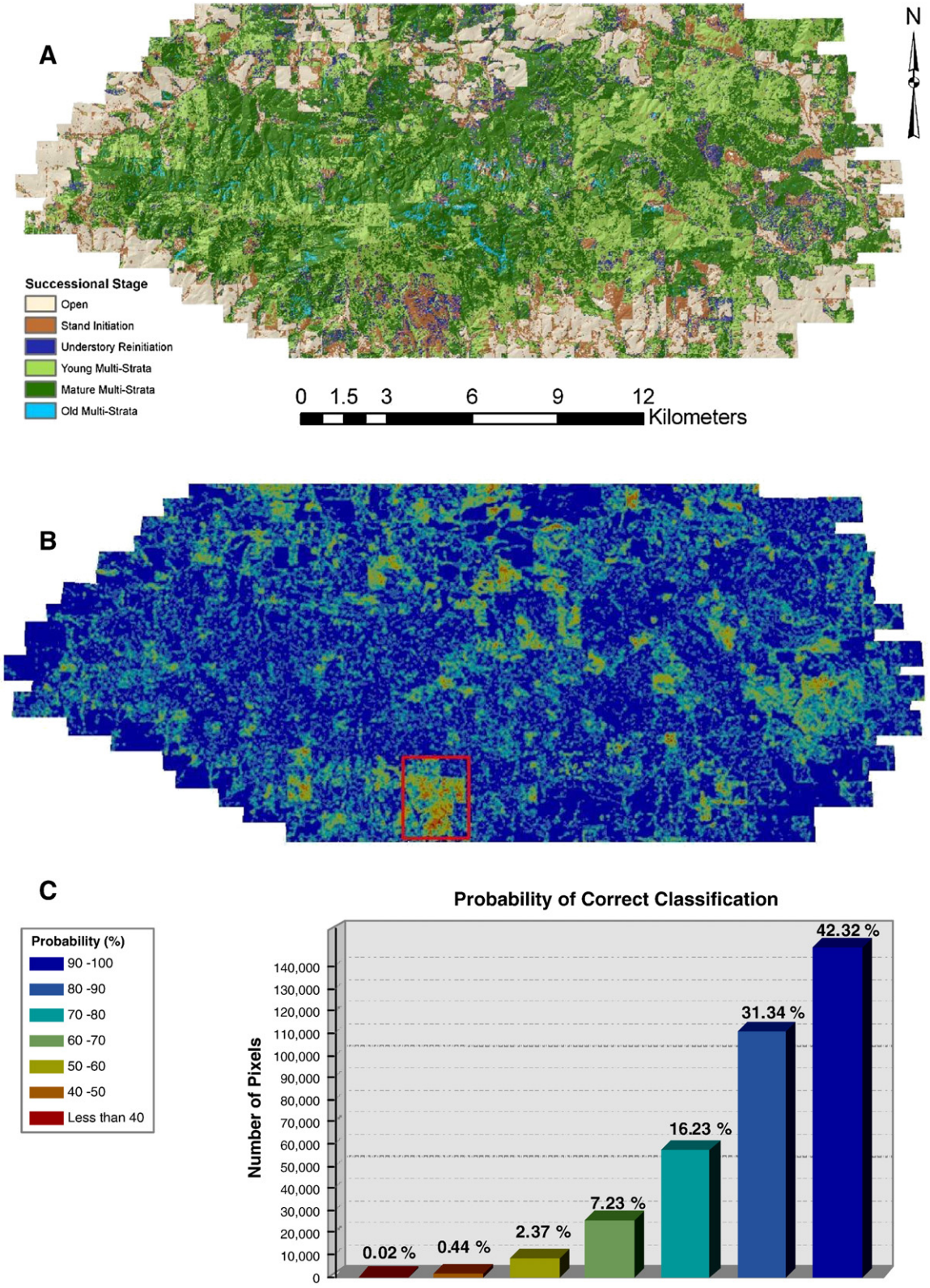

Fig. 6. (A) Successional stage classification map. (B) Maximum probability (classification uncertainty) map. The red box corresponds to the area of detail presented in Fig. 7. (C) Classification uncertainty statistics. The color of each bar corresponds to the associated certainty level in the legend. The percentages listed above each bar are the percentage of total land area occupied by each probability class across the study area.

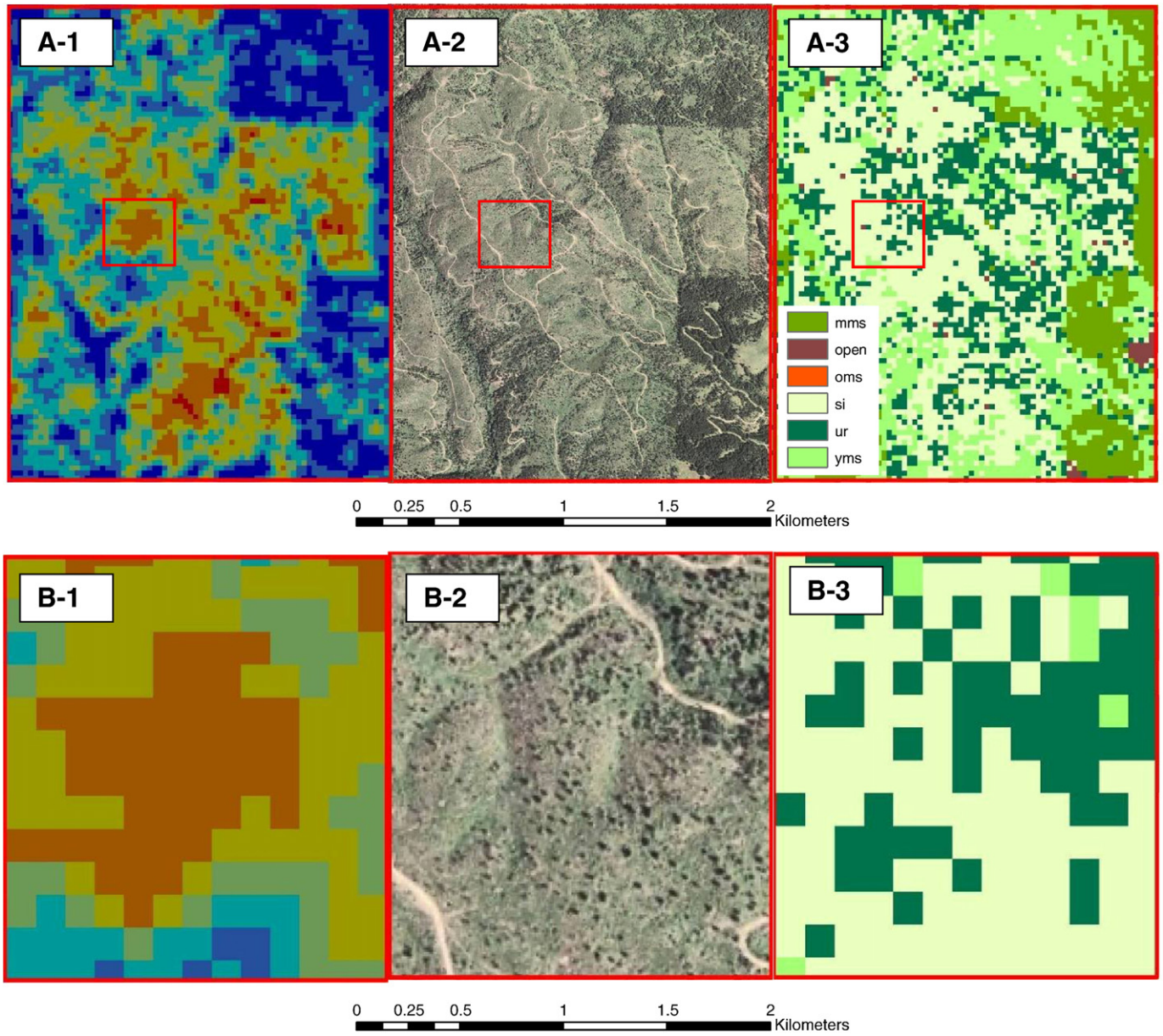

Fig. 7. Detailed view of area with low levels of classification certainty. A-1, A-2, and A-3 are the uncertainty map, aerial photo, and succession classification, respectively. The red box in A-1:A-3 corresponds to the area of detail provided in B-1:B-3.

(Fig. 6A), indicates that most of the study area (~75%) has a classification confidence greater than 80%. Furthermore, only 3% of the total area has classification confidence less than 60% (Fig. 6C). In general, visual interpretation of high spatial resolution ortho-photography indicates that the highest classification uncertainties occur in recently harvested areas exhibiting a high degree of structural variability (Fig. 7).

4. Discussion

The accuracies of the classifications presented in this study are similar to or higher than those attained in other studies classifying forest succession from remotely sensed data. For example, Falkowski et al. (2005) classified four different successional stages across the Palouse Range with ASTER imagery and attained an overall accuracy of only 68.4%. In terms of classifying forest succession from lidar data, Zimble et al. (2003) reported an overall accuracy of 97% when differentiating between two forest successional stages, while Hill and Thomson (2005) achieved an overall accuracy of 94% when classifying ten different structurally based vegetation type classes from a dataset integrating hyperspectral imagery and lidar data. The current study demonstrates that lidar data alone can be used to accurately classify multiple stages of forest succession across fairly large spatial extents (a ~30,000 ha study area).

Inter-class error rates were relatively low for most of the forest successional stages classified in this study (Tables 3 and 4). However, in the seven-class model, the CSE and MMS categories had a relatively high degree of confusion. This is not surprising given their structural similarities. The only structural difference between these two classes is the presence and absence of seedlings or saplings in the understory. It is also useful to point out that the algorithmic modeling procedure selected five lidar metrics for the six-class successional stage classification, while eight variables were identified for the seven-class model. These results suggest that the characteristics of the lidar data used in this study, or the metrics that were used, were not sufficiently able to differentiate seedling and saplings from other

understory components (*e.g.*, shrubs, downed woody debris). Furthermore, in closed canopy forests there is a significant reduction in the number of lidar pulses that reach the forest understory, further inhibiting the direct characterization of understory components via lidar data (Goodwin, 2006; Goodwin et al., 2007; Lee et al., 2004). Considering the importance of understory for evaluating forest management activities (Kozlowski, 2002), understanding forest regeneration (Lormier et al., 1994), and characterizing wildlife habitat (Brokaw & Lent, 1999), further research should explore alternative methods for modeling understory vegetation. This could perhaps be facilitated by developing new lidar metrics specifically focused on quantifying forest understories, or by including other classification variables that influence the occurrence of understory vegetation (*e.g.*, variables quantifying topographic gradients and/or canopy light interception).

The RF classification algorithm utilized in this study produced accurate classifications and provided a means to assess the relative importance of each lidar height metric used to classify forest successional stage. Of the thirty-four candidate lidar height metrics, only nine unique variables were selected as being important in both the seven- and six-class forest succession models (Table 2). Of these nine variables, canopy cover and mean lidar height were selected as the most important variables in both the seven- and six-class forest succession model. The conditional density plots (Figs. 4 and 5) demonstrate that the RF algorithm produced logical, ecologically meaningful classifications. For the seven- and six-class models, the peak of the conditional density plot of the mean lidar height metric increases as forests transition from early to advanced stages of succession. This trend reflects the vertical growth of forests through the successional time sequence. Canopy cover displays a similar trend; as succession advances canopy cover increases. However, when the forest is transitioning into the OMS class there is a slight reduction in canopy cover, representing the creation of canopy gaps as old trees undergo mortality. In addition to providing insight into RF classification rules, the conditional density plots provide a means of assessing potential sources of classification error. For example, in the seven-class model, there is substantial overlap in the probability density function of the mean lidar height metric between the MMS and CSE classes. There is also substantial overlap in the canopy cover probability density function between these classes (Fig. 4). The overlap in these metrics is one potential reason that the MMS and CSE classes exhibit a relatively large amount of confusion.

In terms of the final classification confidence, the maximum probability of occurrence map indicates that low classification confidences typically occur in recently harvested areas across the entire study area. This may be due to high structural variability in these areas (*i.e.*, small patches of trees interspersed with large open areas). High structural variability across small spatial extents could result in 20 m grid cells (*i.e.*, lidar bins) that have mixed-class membership, analogous to a mixed pixel in optical remotely sensed data. It is also worth noting that the classification confidence map presented herein simply highlights areas where there is high uncertainty in classification accuracy, but that high uncertainty does not necessarily indicate incorrect classification. For example, the information provided in Fig. 7 indicates that, although there is a high classification uncertainty, the RF algorithm is correctly classifying the recently harvested area as initiating, young, or regenerating forest.

Although classification accuracies attained via lidar were higher than previous studies classifying forest successional stage from multispectral data alone, it is worth pointing out that that these instruments operate at completely different scales. Classifying forest successional stage at regional to continental scales via discrete return lidar data would be cost prohibitive. However, multispectral data could be employed to produce forest successional stage classifications at these scales. Forthcoming spaceborne lidar missions such as NASA's DESDynI, ICESat-II, and LIST may provide a means to characterize and monitor forest successional stages at global scales. However, before this is feasible research should be conducted to develop and evaluate methods for classifying forest successional stage from large footprint lidar systems.

5. Conclusions

We evaluated the efficacy of lidar height metrics to classify forest successional stage across a structurally diverse, mixed-species forest of the Inland Northwest, USA. Specifically, we hypothesized that a classification algorithm employing a suite of lidar height metrics characterizing the three-dimensional structure of forest canopies would enable forest successional stage to be mapped with a high accuracy. Indeed, the successional stage classifications presented herein achieved overall accuracies higher than 90% (overall accuracies for the seven-class and six-class models were 90.1% and 95.5%, respectively). These results demonstrate that lidar data alone can accurately characterize forest succession across large spatial extents.

The classifications produced in this study will be used to achieve multiple sustainable forest management goals. Specifically, work is currently underway to utilize the three-dimensional vegetation structure information presented herein to advance the characterization and modeling of wildlife habitats (see Vierling et al., 2008). This work includes investigating the utility of lidar and topographic metrics to quantify understory characteristics and other forest attributes important for wildlife habitat assessment. Furthermore, the forest successional stage classification will be used to parameterize a forest succession model so that forest succession dynamics can be modeled, with the ultimate goal of understanding the impact different management regimes have upon future carbon storage in the forest.

Acknowledgements

This work was primarily supported through Agenda 2020's sustainable forestry initiative via a grant provided by the USDA Forest Service Rocky Mountain Research Station, Moscow Forest Sciences Laboratory (RJVA-11222063-299). The authors would like to acknowledge multiple additional sources of funding and support for this work including: the USDA Forest Service Rocky Mountain Research Station Missoula Fire Sciences Laboratory (RJVA-11222048-140), the NASA Synergy program, the United States Geological Survey's GAP Analysis Program, the USDA Forest Service International Institute of Tropical Forestry, and the University of Idaho's Geospatial Laboratory for Environmental Dynamics. We also thank four anonymous reviewers for their input and comments on an earlier version of this manuscript.

References

Bergen, K. M., & Dronova, I. (2007). Observing succession on aspen-dominated landscapes using a remote sensing-ecosystem approach. *Landscape Ecology*, *22*, 1395−1410.
Breiman, L. (2001). Random Forests. *Machine Learning*, *45*, 5−32.
Breiman, L., Friedman, J. H., Olshen, R. A., & Stone, C. J. (1984). *Classification and regression trees.* Monterey, CA: Wadsworth and Brooks/Cole.
Brokaw, N. V., & Lent, R. A. (1999). Vertical structure. In M. Hunter (Ed.), *Maintaining Biodiversity in Forest Ecosystems* (pp. 373−399). Cambridge: Cambridge University Press.
Busing, R. T., Solomon, A. M., McKane, R. B., & Burdick, C. A. (2007). Forest dynamics in Oregon landscapes: Evaluation and application of an individual-based model. *Ecological Applications*, *17*, 1967−1981.
Clark, D. B., Olivas, P. C., Oberbauer, S. F., Clark, D. A., & Ryan, M. G. (2008). First direct landscape-scale measurement of tropical rain forest Leaf Area Index, a key driver of global primary productivity. *Ecology Letters*, *11*, 163−172.
Cody, M. L. (1985). *Habitat selection in birds.* New York: Academic Press.
Cohen, W. B., Spies, T., & Fiorella, M. (1995). Estimating the age and structure of forests in a multi-ownership landscape of western Oregon, U.S.A.. *International Journal of Remote Sensing*, *16*, 721−746.
Coops, N. C., Hilker, T., Wulder, M. A., St-Onge, B., Newnham, G., Siggins, A., et al. (2007). Estimating canopy structure of Douglas-fir forest stands from discrete-return lidar. *Trees*, *21*, 295−310.

Coops, N. C., Wulder, M. A., & White, J. C. (2006). Integrating remotely sensed and ancillary data sources to characterize a mountain pine beetle infestation. *Remote Sensing of Environment*, *105*, 83—97.
Cutler, R. D., Edwards, T. C., Jr., Beard, K. H., Cutler, A., Hess, K. T., Gibson, J., et al. (2007). Random Forests for classification in ecology. *Ecology*, *88*, 2783—2792.
Deguchi, A., Hattori, S., & Park, H. T. (2006). The influence of seasonal changes in canopy structure on interception loss: Application of the revised Gash model. *Journal of Hydrology*, *318*, 80—102.
Dubayah, R. O., & Drake, J. B. (2000). Lidar remote sensing for forestry. *Journal of Forestry*, *98*, 44—46.
Evans, J. S., & Hudak, A. T. (2007). A multiscale curvature algorithm for classifying discrete return lidar in forested environments. *IEEE Transactions on Geoscience and Remote Sensing*, *45*, 1029—1038.
Falkowski, M. J., Gessler, P. E., Morgan, P., Hudak, A. T., & Smith, A. M. S. (2005). Evaluating ASTER satellite imagery and gradient modeling for mapping and characterizing wildland fire fuels. *Forest Ecology and Management*, *217*, 129—146.
Fuller, R. J., Smith, K. W., Grice, P. V., Currie, F. A., & Quine, C. P. (2007). *IBIS*, *149*, 261—268.
Gentle, J. E., Hardle, W., & Mori, Y. (2005). *Handbook of Computational Statistics.* American Statistical Association.
Golub, G. H., & Van Loan, C. F. (1996). *Matrix Computations*, 3rd ed. : Johns Hopkins.
Goodwin, N.R. (2006). Assessing Understorey Structural Characteristics in Ecucalyptus Forests: an investigation of lidar techniques (Thesis). University of New South Wales, Sydney NSW Australia (206 pp.).
Goodwin, N. R., Coops, N. C., Bater, C., & Gergel, S. E. (2007). Assessment of sub-canopy structure in a complex coniferous forest. *ISPRS Workshop on Laser Scanning and SilviLaser 2007, Espoo, September 12–14, 2007, Finland*.
Hao, Z., Zhang, J., Song, B., Ye, J., & Li, B. (2007). Vertical structure and spatial associations of dominant tree species in an old-growth temperate forest. *Forest Ecology and Management*, *252*, 1—11.
Helle, P. (1985). Effects of forest regeneration on the structure of bird communities in northern Finland. *Holarctic Ecology*, *8*, 120—132.
Helle, P., & Monkkonen, M. (1990). Forest successions and bird communities: Theoretical aspects and practical implications. In A. Keast (Ed.), *Biogeography and ecology of forest bird communities* (pp. 299—318). The Netherlands: SPB Acedemic Publishing.
Hill, R. A., & Thomson, A. G. (2005). Mapping woodland species composition and structure using airborne spectral and lidar data. *International Journal of Remote Sensing*, *26*, 3763—3779.
Hudak, A. T., Crookston, N. L., Evans, J. S., Falkowski, M. J., Smith, A. M. S., Gessler, P., et al. (2006). Regression modeling and mapping of coniferous forest basal area and tree density from discrete-return lidar and multispectral satellite data. *Canadian Journal of Remote Sensing*, *32*, 126—138.
Hudak, A. T., Crookston, N. L., Evans, J. S., Hall, D. E., & Falkowski, M. J. (2008). Nearest neighbor imputation modeling of species-level, plot-scale structural attributes from lidar data. *Remote Sensing of Environment*, *112*, 2232—2245.
Kozlowski, T. T. (2002). Physiological ecology of natural regeneration of harvested and disturbed forest stands: Implications for forest management. *Forest Ecology and Management*, *158*, 195—221.
Law, B. E., Cescatti, A., & Baldocchi, D. D. (2001). Leaf area distribution and radiative transfer in open-canopy forests: Implications for mass and energy exchange. *Tree Physiology*, *21*, 777—787.
Lawrence, R. L., Wood, S. D., & Sheley, R. L. (2006). Mapping invasive plants using hyperspectral imagery and Breiman Cutler classifications (RandomForest). *Remote Sensing of Environment*, *100*, 356—362.
Lawrence, R. L., & Wright, A. (2001). Rule-based classification systems using classification and regression tree (CART) analysis. *Photogrammetric Engineering and Remote Sensing*, *67*, 1137—1142.
Lee, A., Lucas, R.M. & Brack, C. (2004). Quantifying vertical forest stand structure using small footprint lidar to assess potential stand dynamics. Proceedings, NATSCAN — Laser scanners for forest and landscape assessment instruments, processing methods and applications 3–6 October, Freiburg, Germany. *International Archives of Photogrammetry, Remote Sensing and Spatial Information Sciences*, 36, 213–217.
Lefsky, M. A., Harding, D., Cohen, W. B., & Parker, G. G. (1999). Surface lidar remote sensing of the basal area and biomass in deciduous forests of eastern Maryland, USA. *Remote Sensing of Environment*, *67*, 83—98.
Liaw, A., & Wiener, M. (2002). Classification and regression by Random-Forest. *R News*, *2*, 18—22.
Lormier, C. G., Chapman, J. W., & Lambert, W. D. (1994). Tall understorey vegetation as a factor in the poor development of oak seedlings beneath mature stands. *Journal of Ecology*, *82*, 227—237.
Miller, J. D., Danzer, S. R., Watts, J. M., Stone, S., & Yool, S. R. (2003). Cluster analysis of structural stage classes to map wildland fuels in a Madrean ecosystem. *Journal of Environmental Management*, *68*, 239—252.
Nelson, R. F., Krabill, W. B., & Tonelli, J. (1988). Estimating forest biomass and volume using airborne laser data. *Remote Sensing of Environment*, *24*, 247—267.
O'Hara, L. O., Latham, P. A., Hessburg, P., & Smith, B. G. (1996). A structural classification for inland Northwest forest vegetation. *Western Journal of Applied Forestry*, *11*, 97—102.
Pocewicz, A., Gessler, P. E., & Robinson, A. P. (2004). The relationship between leaf area index and Landsat spectral response across elevation, solar insolation, and spatial scales, in a northern Idaho forest. *Canadian Journal of Forest Research*, *34*, 65—480.
Prasad, A. M., Iverson, L. R., & Liaw, A. (2006). Newer classification and regression tree techniques: Bagging and random forests for ecological prediction. *Ecosystems*, *9*, 181—199.
R Development Core Team (2007). *R: A language and environment for statistical computing.*Vienna, Austria: R Foundation for Statistical Computing3-900051-07-0 http://www.R-project.org
Roberts, S. D., Dean, T. J., Evans, D. L., McCombs, J. W., Harrington, R. L., & Glass, P. A. (2005). Estimating individual tree leaf area in loblolly pine plantations using lidar-derived measurements of height and crown dimensions. *Forest Ecology and Management*, *213*, 54—70.
Roland, J., & Taylor, P. D. (1997). Insect parasitoid species respond to forest structure at different spatial scales. *Nature*, *386*, 710—713.
Saatchi, S. S., Houghton, R. A., Alvala, R. C. D. S., Soares, J. V., & Yu, Y. (2007). Distribution of aboveground live biomass in the Amazon basin. *Global Change Biology*, *13*, 816—837.
Shugart, H. H. (2000). The importance of structure in the longer-term dynamics of ecosystems. *Journal of Geophysical Research — Atmospheres*, *105*, 20065—20075.
Song, C., Schroeder, T. A., & Cohen, W. B. (2007). Predicting temperate conifer forest successional stage distributions with multitemporal Landsat Thematic Mapper imagery. *Remote Sensing of Environment*, *106*, 228—237.
Song, C., & Woodcock, C. E. (2002). The spatial manifestation of forest succession in optical imagery: The potential of multiresolution imagery. *Remote Sensing of Environment*, *82*, 271—284.
Vargas, R., Allen, M. F., & Allen, E. B. (2008). Biomass and carbon accumulation in a fire chronosequence of a seasonally dry tropical forest. *Global Chance Biology*, *14*, 109—124.
Vierling, K. T., Vierling, L. A., Martinuzzi, S., Gould, W., & Clawges, R. (2008). Lidar: Shedding new light on habitat modeling. *Frontiers in Ecology and the Environment*, *6*, 90—98.
White, M. A., Asner, G. P., Nemani, R. R., Privette, J. L., & Running, S. W. (2002). Measuring fractional cover and leaf area index in arid ecosystems: digital camera, radiation transmittance, and laser altimetry methods. *Remote Sensing of Environment*, *74*, 45—57.
Zimble, D. A., Evans, D. L., Carlson, G. C., Parker, R. C., Grado, S. C., & Gerard, P. D. (2003). Characterizing vertical forest structure using small footprint airborne lidar. *Remote Sensing of Environment*, *87*, 171—182.